International Conference on HAZARDOUS WASTE : Sources, Effects and Management
12-16 December 1998, Cairo-Egypt

T-1

Removal of Contaminants from Waste Streams at Gas Evolving Flow-Through Porous Electrodes

Mahmoud M. Saleh
Department of Chemistry, Faculty of Science, Cairo University, Egypt

Abstract

Electrochemical techniques have been used for the removal of inorganic and organic toxic materials from industrial waste streams. One of the most important branch of these electrochemical techniques is the flow-through porous electrode. Such systems allow for the continuous operation and hence continuous removal of the contaminants from waste streams at high rates and high efficiency. However, when there is an evolution of gas bubbles with the removal process, the treatment process needs a much different treatment of both the design and the mathematical treatment of the such these systems. The evolving gas bubbles within the electrode decrease the pore electrolyte conductivity of the porous electrodes, decrease the efficiency and make the current more non-uniform. This cause the underutilization of the reaction area and finally make the electrode inoperable. In this work the harmful effects of the gas bubbles on the performance of the porous electrode will be modeled. The model accounts for the effects of kinetics, mass transfer and gas bubbles resistance on the overall performance of the electrode. This will help in optimizing the operating conditions and the cell design.

Keywords : Waste Streams/ Flow-Through/ Porous Electrode/ Gas Evolution/ Mathematical Model.

Introduction

Electrochemical gas evolution continues to occupy an important role in many important technological, industrial and environmental problems. Gas evolving electrodes are characterized by complicated behavior of the electrolytic bubbles which give rise to numerous effects on the cell performance. While it is difficult to separate these effects experimentally, theoretical analysis can sometimes help to identify trends and suggesting improvements[1]. A large number of publications has been found in the effects of evolving gas bubbles on the polarization and current distributions and on the mechanism of mass transfer at planar electrodes[2-6]. However, they have not been fully quantified in porous electrodes. Coleman *et al.*[7] modeled the reduction of nitrate and nitrite ions from nuclear waste streams at parallel plate flow reactor. They studied the effects of the evolving gases on the performance of the cell process. Although the destruction of nitrate and nitrite ions to gaseous products is an important process to be studied at porous electrodes, yet, the present model will be a rather general model. The scope of the present work is restricted to the gas evolution at flow-through porous electrodes when the gas reaction is mass transfer controlled.

Flow-through porous electrodes are characterized by both high specific reaction area per unit volume and low mass transfer resistance. The theory behind the operation of porous electrodes has been developed to sophisticated levels; several reviews have been published on the theory and applications of these systems[8-11]. Flow-through porous electrodes have been used in

electrosynthesis [12, 13], charging and discharging of redox batteries for load leveling applications [14, 15], removal and recovery of heavy metals from waste streams [16-22] and destruction and removal of cyanide wastes from electroplating baths [23]. The gas evolution reaction at porous electrodes require different design and operating considerations since the unavoidable generation of gas bubbles within the pores can eventually render the electrode inoperable. The evolving gas bubbles accumulate within the pores leading to a significant increase in the pore electrolyte resistivity [24].

Ateya and El-Anadouli [24, 25] modeled the effects of the evolution of hydrogen gas bubbles within the pores on the current and potential distributions within flow-through porous electrodes and on their overall polarization behavior. This case was for a single electrode reaction under no mass transfer control. Saleh *et al.*, [26] recently modeled the effects of the evolved hydrogen gas bubbles on the current distributions and the efficiency of the electrowinning of non-noble metals at flow-through porous electrodes. These models [24, 25 and 26] treated the hydrogen gas evolution reaction which is not mass transfer controlled but it is rather kinetically and ohmically controlled. More recently, White and Pauline [27] developed a general system of governing equations for transport in porous electrodes include three phases; solid, liquid and gas. They did not introduce any results, solutions or analyses for that system.

The simulation presented in this work help us to determine the effects of the operational parameters on the cell efficiency for a given set of structural, transport and/or kinetic parameters of the system. These information can be used to guide the cell design and optimize the operational conditions of the process.

Mathematical Model

Figure (1) shows a schematic diagram of the packed bed compartment, counterelectrode and direction of electrolyte flow. The place of the counterelectrode was chosen to be downstream to avoid the problems associated with the gas bubbles which are generated excessively at the polarized face of the working electrode and which were not taken into consideration in previous studies [26,28,29].

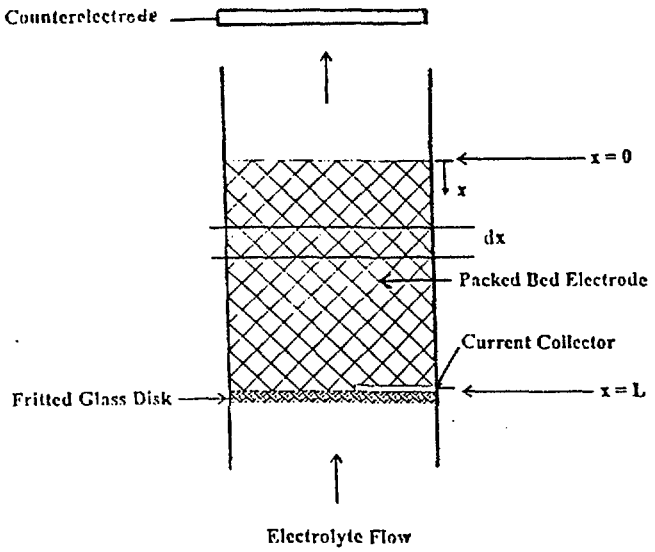

Fig. (1) Schematic of the electrolytic cell.

The reaction considered here is the reduction of ionic species to gaseous product at the flow- through porous cathode. The model is developed under the following assumptions:
1. Ionic migration and axial diffusion and dispersion effects are negligible.
2. The packed bed electrode has uniform porosity and sufficiently high electronic conductivity compared to that of the electrolyte, such that the potential gradient within the solid phase of the packed bed can be neglected. The packed bed is also assumed to be made of an inert substrate and characterized by a porosity, θ.
3. Butler-Volmer equation governs the kinetics of the reaction which involves a two electron transfer rate-determining step. The reaction is first order in the active ion concentration.
4. The mass transfer resistance is due to a stagnant diffusion layer at the electrode-electrolyte interface within the pore structure, i.e. around the circumference of the packing particles [30].
5. The model is formulated for steady state operation with low conversion efficiency per single pass, *i.e.*, there are negligible changes in the concentration of the ions in the axial direction of convective flow.

In view of assumption 3, a modified Butler-Volmer equation correlates the solution current, i(x) with the reaction current, j(x) by, (see Ref. 26),

$$\frac{di(x)}{dx} = -j(x) = \frac{-Si_o[1-\exp(2\eta(x)/b)]}{\exp[\beta\eta(x)/b] + \frac{i_o}{i_L}} \qquad [1]$$

The local limiting current density, i_L is related to the local mass transfer coefficient, k_m and the bulk concentration, C by,

$$i_L = nFk_mC \qquad [2]$$

Empirical correlations for the local mass transfer coefficient, k_m can be obtained from literature [31,32].

Ohm's law and in view of assumption 2, relates the solution current travels through the gas-electrolyte dispersion filling the pore space with the change in polarization. Therefore,

$$i(x) = \kappa(x)\frac{d\eta(x)}{dx} \qquad [3]$$

The conductivity of the gas-electrolyte dispersion within the pores, $\kappa(x)$, is a complex function involving the composition of the electrolyte, the porosity of the bed and the void fraction of the gas filling the pore electrolyte, ϵ. For this study, Bruggeman's equation is used as an expression to correlate the conductivity of the gas-electrolyte dispersion which fills the pore space with the gas void fraction [33], *i.e.*,

$$\kappa(x) = \kappa^o[\theta-\epsilon(x)]^{3/2} \qquad [4]$$

where, κ^o is the bulk electrolyte conductivity and $\epsilon(x)$ is the gas void fraction. The latter is given by, [26]

$$\epsilon(x) = \frac{\theta\, i(x)}{Q\,\gamma + i(x)} \qquad [5]$$

where γ is a conversion factor of the current to the volume of gas generated. Assuming ideal gas behavior, γ is given by,

$$\gamma = \frac{2PF}{RT} \qquad [6]$$

where γ equals 7.87 C/cm^3 at standard pressure and temperature.

A system of four equations (Eqs. [1, 3-5]) describing the distributions of four variables, i.e., i, η, ϵ and κ is obtained.

In order to minimize the number of the parameters and to obtain results of general applicability, the variables in the governing equations are put in dimensionless forms. Thus,

$$\frac{d\bar{i}(y)}{dy} = -\bar{j}(y) = \frac{-\left(1 - \exp[2\,\bar{\eta}(y)]\right)}{\left(\exp[\beta\,\bar{\eta}(y)] + \dfrac{I_o}{I_L}\right)} \qquad [7]$$

$$\frac{d\bar{i}(y)}{dy} = K\,\bar{\kappa}(y)\,\frac{d\bar{\eta}(y)}{dy} \qquad [8]$$

$$\bar{\kappa}(y) = [\theta - \epsilon(y)]^{3/2} \qquad [9]$$

$$\epsilon(y) = \frac{\theta\,\bar{i}(y)}{\bar{i}(y) + \Psi} \qquad [10]$$

where $y = x/L$, is the dimensionless distance and the variables with overbars denote normalized variables, i.e., $\bar{i}(y) = i(x)/I_o$, $\bar{\eta}(y) = \eta(x)/b$ and $\bar{\kappa}(y) = \kappa(x)/\kappa^\circ$. Where $I_o = i_o SL$. Four dimensional and dimensionless groups result from this normalization. Table (1) lists them, along with the porosity of the bed and the charge transfer coefficient of the reaction. The physical significance of these groups were discussed in details in Ref. 26. The difference is that in Ref. 26 we normalized the solution current, i with respect to the cell current while as in this model the solution current is normalized with respect to the exchange current density, I_o. The definitions and limits of the groups were changed but they still have their physical significance discussed in Ref. 26.

Table (1) : The dimensionless groups and parameters

Group	Definition
Total exchange current density	$I_o = i_o SL$
Total limiting current	$I_L = i_L SL$
Dimensionless conductivity group	$K = \kappa^\circ b / I_o L$
Dimensionless bubble group	$\Psi = 2PFQ/I_o RT$
Porosity	θ
Charge transfer coefficient	β

Since the physical significance of the dimensional group, I_L and the dimensionless bubble group, Ψ is essential for the present study, their physical significance and limits will be discussed here. The dimensional group, $I_L = i_L SL$ is the effective limiting current supported by the total internal surface area of the bed. The value of I_L determines the significance of the mass transfer resistance on the reaction. Low values of I_L correspond to mass transfer controlled reaction. The dimensionless bubble group, $\Psi = Q\gamma / I_o$ measures the ratio of the electrolyte flow rate to the total exchange current density. Small values of Ψ indicate significant bubble formation. This is obtained under conditions of low electrolyte flow rates and/or high I_o.

The boundary conditions are :

$y = 0$, $\bar{i} = i_{cell}/I_o$

$y = 1$, $\bar{i} = 0$, $d\bar{\eta}/dy = 0$, $\bar{\kappa} = \theta^{1.5}$ and $\epsilon = 0$

The four variables ($\bar{i}$, $\bar{\eta}$, ϵ, $\bar{\kappa}$) and the model equations (Eqs.[7-10]) were solved using a finite difference algorithm developed by Newman [34].

Results and Discussions

The above system of equations combines the effects of the charge transfer kinetics, mass transfer, ohmic resistance and gas bubbles on the overall polarization behavior and on the distributions of the gas void fraction, pore electrolyte conductivity, polarization and reaction currents within the porous electrode. Since the effects of the kinetics and ohmic resistances were studied in previous works [24,25], this study is restricted to the combined mass transfer and bubble formation effects. The model, however, will be solved and discussed under two cases:
- the first; independent variation of mass transfer resistance and bubble formation,
- and the second is the combined effects of both mass transfer resistance and bubble formation.
The second case will be introduced as a case study. This will help to explore the physical significance of the model predictions.

Independent variation of mass transfer resistance and bubble formation — The generated gas bubbles decrease the cross-sectional area available for ionic flow, and consequently decrease the effective conductivity of the pore electrolyte. (see Eqs. [4, 9]). The effects of the mass transfer resistance and the bubble formation were quantified by solving the dimensionless model, i.e., Eqs. [7-10] simultaneously. For all the calculations presented in this work, the value of the porosity, θ and the charge transfer coefficient, β are taken to be 0.7 and 1, respectively.

Figure (2) shows the effect of the dimensionless bubble group, Ψ , on the distribution of the gas void fraction, $\epsilon(y)$ and on the distribution of the pore electrolyte conductivity, $\bar{\kappa}(y)$, at a value of the dimensionless conductivity group, K = 10, cell current = 0.2 A cm^{-2}, total exchange current density, I_o = 0.02 A cm^{-2}, and total mass transfer limiting current, I_L = 10 A cm^{-2}. I_L has a large value such that the value I_o/I_L in Eq. [7] is eliminated. This is a case of negligible mass transfer resistance. This helps to identify the values of Ψ where the bubble formation is significant and the values of Ψ where the bubble formation is negligible.

It is clear from the figure that as the magnitude of Ψ decreases, the gas void fraction increases and a significant amount of gas bubbles can accumulate at the polarized (front) face of the electrode at values of $\Psi < 4$. At sufficiently low Ψ values (e.g., $\Psi = 0.4$), virtually more than 50% of the entire thickness of the bed is plugged with gas bubbles. This corresponds to low electrolyte flow rates, Q or high exchange current density, I_o. This causes a large increase in the gas void fraction through most of the thickness of the electrode. The effect of Ψ on the gas void fraction is reflected on the dimensionless pore electrolyte conductivity, $\bar{\kappa}(y)$ as shown in Fig. (2). As Ψ decreases, $\bar{\kappa}(y)$ decreases. At high value of Ψ, the dimensionless conductivity of the electrolyte is constant through out the bed and equals to $\theta^{1.5}$ which is corresponding to negligible bubble formation. For low values of Ψ, most of the electrode is plugged with the bubbles and pore electrolyte conductivity has lower values.

Figure (3) shows the effect of the dimensionless bubble group, Ψ, on the potential of the reduction reaction at K = 10 and cell current = 0.2 A cm^{-2}. As Ψ decreases the potential reaction current becomes more non-uniform. As Ψ decreases the gas void fraction increases leading to a decrease in the pore electrolyte conductivity. This results in a non-uniform potential distribution which leads to greater localization of the reaction towards the front of the electrode. This points to the deleterious effects of the gas bubbles on the conductivity of the pore

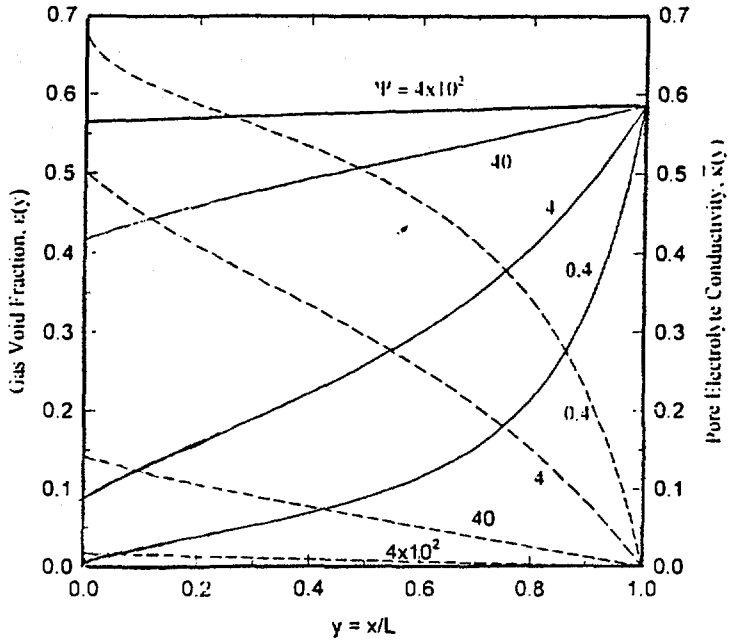

Fig. (2) Effect of the dimensionless bubble group, Ψ on the distributions of the gas void fraction (dashed lines) and the pore electrolyte conductivity (solid lines). K = 10; I_o = 0.02 A cm^{-2} ; I_L = 10 A cm^{-2}.

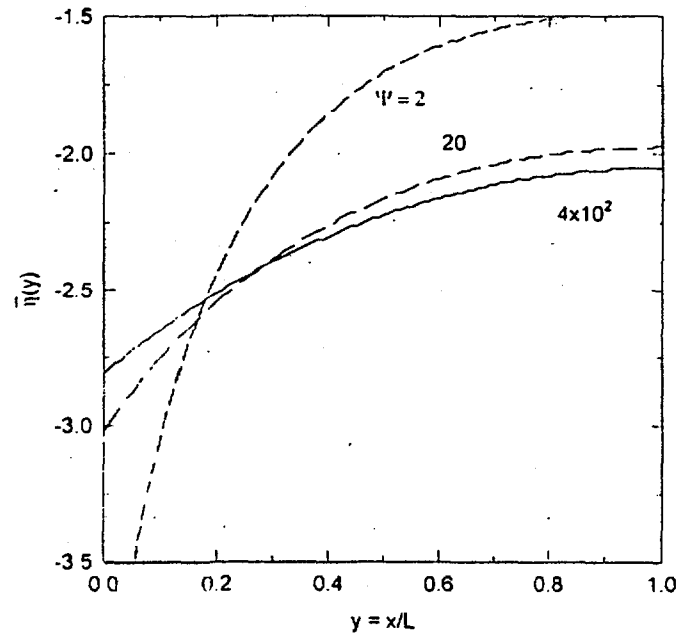

Fig. (3) Effect of the dimensionless bubble group, Ψ on the distributions of the polarization. K = 10; I_o = 0.02 A cm^{-2}.

electrolyte and hence on the current and potential distributions. For large values of Ψ i.e., $\Psi > 4x10^2$, the gas void fraction is relatively small (see Fig. (2)), and the distribution of the reaction is more uniform pointing to a negligible bubble effects. The above results are consistent with the results found in previous work [24]. However, the quantization of the combined effects of the mass transfer resistance and gas bubble formation is of great practical importance for the gas evolving porous electrodes. This will be discussed in the coming section.

Figure (4) shows the effects of the bubble group, Ψ on the relations between dimensionless current and the dimensionless polarization at $I_L = 0.1$ A cm^{-2} and K = 1. As the polarization increases the current increases until it reaches to a limiting current the value of which depends on the value of the dimensionless bubble group, Ψ. At low values of Ψ, an excessive amount of gas bubbles are produced within the electrode resulting in non-uniform polarization. Hence, the reaction is localized in a thin layer near the polarized (front) face of the electrode. Under these conditions the local mass transfer limitation is significant and the predicted total limiting current is much lower than the theoretical limiting current. Note that there is no significant difference between the i-E relations of the cases where $\Psi = 40$ and $4x10^2$ owing to the negligible bubble formation (see Fig. (2)). This point can be further explained by studying the current distribution under mass transfer control and at significant formation of gas bubbles.

Figure (5) shows the reaction current distributions at different values of the total limiting current, I_L. As I_L increases, the current distribution becomes more non-uniform. This is because the gas is evolved preferentially at the front of the electrode and the reaction becomes more ohmically controlled and hence less uniform. Since the model treats the case of low single pass conversion efficiency, hence the axial concentration is uniform but not the potential. Therefore, ohmic effects cause the reaction to be non-uniform at high I_L. However, at low values of I_L, the reaction is mass transfer controlled and hence it is more uniform. Note that at $I_L = 0.5$ A cm^{-2}, the electrode operates at the limiting current in about 20 % only of the available thickness of the electrode. At the front of the electrode, both the excessive gas bubbles (high polarization) and mass transfer resistance cause the current to level off. Therefore, local mass transfer can limit the reaction even when the cell current is well below the total limiting current.

Combined Effects of mass transfer resistance and bubble formation -Case study -In practice the electrolyte flow rate, Q affects both the total limiting current, I_L and the dimensionless bubble group, Ψ with different degrees. Thus, it is more realistic to explore the effects of the flow rate separately on the cell performance. The bubble group, Ψ is a linear function of the flow rate, Q (see Table (1)), where the mass transfer total limiting current, I_L depends on Q to a power determined by the mass transfer correlation used. For this study, the Colquhoum *et al.* formula [9] was used. In this formula, the mass transfer coefficient, k_m and hence the total limiting current (see Eq.[2]) depends on Q to one sixth power such that,

$$k_m = 0.62\, S\, D \left(\frac{\nu}{D}\right)^{1/3} Re^{1/6} \qquad [11]$$

where *Re* is the Reynolds number and is given by;

$$Re = \frac{Q d}{\nu (1-\theta)} \qquad [12]$$

where ν is the kinematic viscosity of the solution, D is the diffusivity and d is the particle diameter. In combining Eqs. [2, 11 and 12], I_L can be written as;

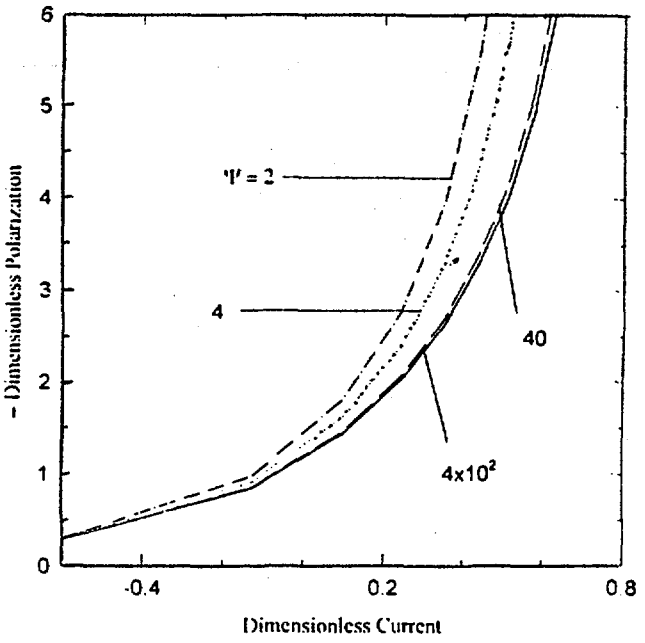

Fig. (4) Effect of the dimensionless bubble group, Ψ on the i-E relations at $I_L = 0.1$ A cm^{-2}, $I_o = 0.02$ A cm^{-2} and K = 1.

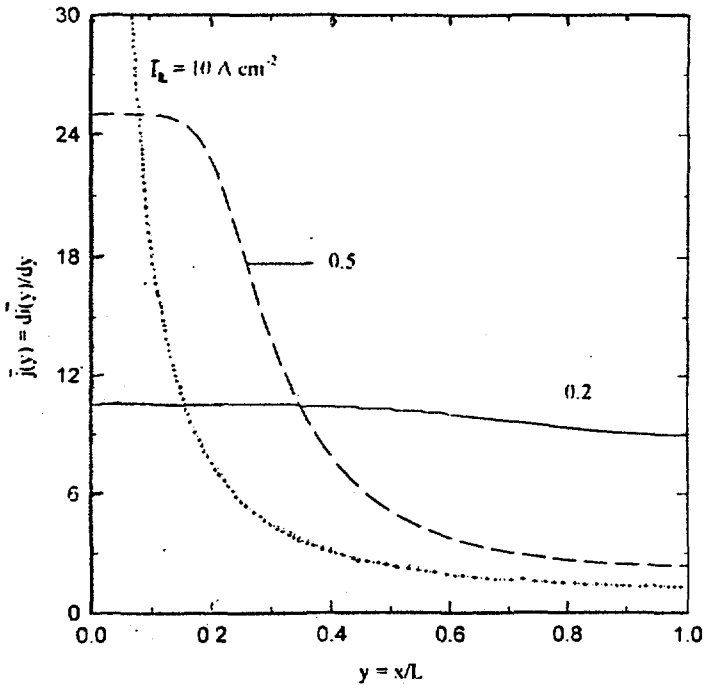

Fig. (5) Effect of gas bubble formation on the reaction current distributions at different values of I_L. K = 1; Ψ = 4; $i_{cell} = 0.2$ Acm^{-2}.

$$I_L = a\, Q^{1/6} \qquad [13]$$

where a is a constant depends on the parameters used in the simulation, such that;

$$a = 0.62 x n F S^2 L D^{2/3} C \left[\frac{d\nu}{(1-\theta)}\right]^{1/6} \qquad [14]$$

For this simulation, C was taken to be 10^{-5} mole/cm^3, d = 0.1 cm, D = $2x10^{-6}$ cm^{2}s^{-1}, L = 5 cm, S = 40 cm^{-1}, and ν = 0.01 cm^2 s^{-1}. Hence, the value of the constant a equals to 0.587.

The dimensionless model is solved under these conditions to explore the effects of the electrolyte flow rate on the reaction current distributions and on the overall performance of the electrode. Figure (6, 7) show the relations between the dimensionless current and the dimensionless polarization at different electrolyte flow rate , Q. Figure (6) shows the case where the gas bubble effects are included in the simulation, whereas, Fig. (7) shows the case where the gas bubble effects are not included. Note that the dimensionless current is the dimensionless cell current which is equal to the dimensionless solution current at the exit face *i.e.*, at y = 0. The dimensionless polarization is the polarization corresponding to the dimensionless current *i.e.*, the polarization at y = 0. The figures reveal the following features:

i- As the polarization increases the current increases until it reaches to a limiting current the value of which depends on the flow rate, Q.

ii- The limiting current values in the case where the gas bubble formation is included (Fig,. (6)) are lower than in the case where the gas bubble formation is not included (Fig. (7)). Note that the bubble group is linearly dependent on Q whereas the theoretical total limiting current depends on Q to a power of sixth. Hence, in Fig. (7) where the model account only for I_L, the values of the predicted limiting currents are higher than that in Fig. (6).

iii- At Q = 1 cm s^{-1}, there is no any significant difference between the two cases which signs to the negligible extent of the bubble formation.

The above point can be further explained by plotting the total limiting current as a function of the flow rate. The results are shown in Fig. (8). The figure shows the predicted limiting current where the bubble formation is included and not included and the theoretical limiting current. The limiting current values were predicted from Figs. (6 and 7) at arbitrary dimensionless polarization of -20. These predicted limiting currents are of the practical interest because to reach to the theoretical limiting current values, one should operate the cell at very high potentials. Under these conditions of high polarization, one should expect high power consumption which overweighs the conditions of operating the cell at the practical limiting currents. Side reaction is also expected to take place at high polarizations. The figure reveals three features:

1. In the case where the gas bubble formation is not included, at low flow rates (Q < 0.1 cm s^{-1}), the values of the predicted limiting currents equal to the theoretical limiting current. At low flow rates the reaction is mass transfer controlled and hence the reaction is uniform and operates at the limiting current everywhere within the electrode. Therefore, the predicted limiting currents equal the theoretical limiting currents.

2. In the case where the gas bubble formation is not included, at high flow rates (Q > 0.1), the estimated limiting currents are lower than the theoretical limiting currents. At high flow rates the reaction is under combined ohmic and mass transfer control. The ohmic effects cause the reaction to be restricted to a thin layer at the front of the electrode (see Fig.. (2)) where the polarization at

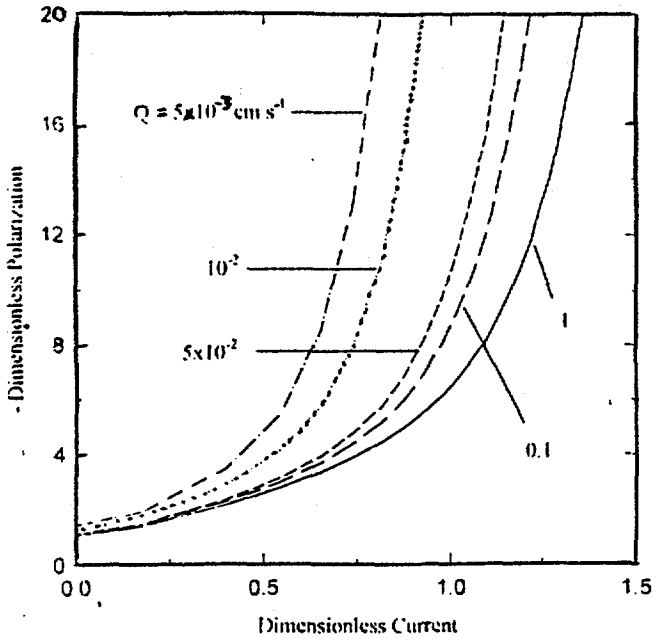

Fig. (6) Effect of the flow rate, Q on the i-E relations. Bubble formation is included in the simulation. K = 1; I_o = 0.02 A cm^{-2}.

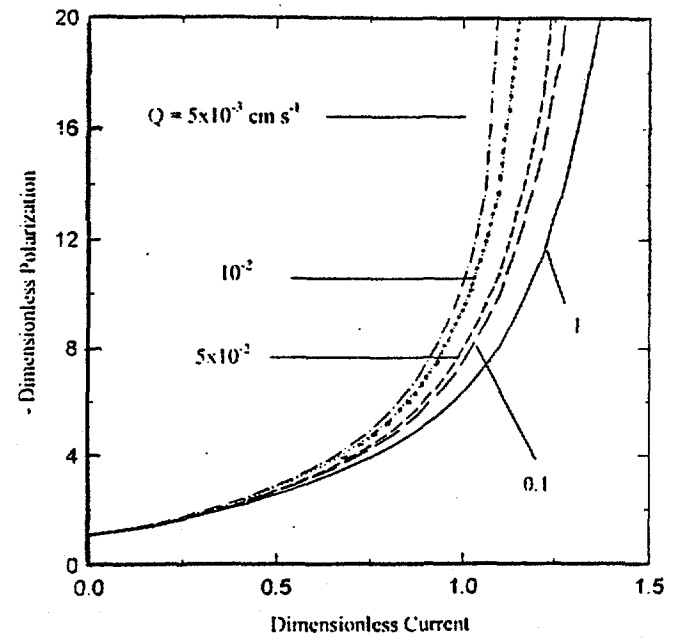

Fig. (7) Effect of the flow rate, Q on the i-E relations. Bubble formation is not included in the simulation. K = 1; I_o = 0.02 A cm^{-2}.

the exit face is high enough to support the limiting current. In this case, the local mass transfer limitation can be significant and limits the reduction reaction and the predicted limiting currents are lower than the theoretical limiting currents.
3. In the case where the bubble formation included, the values of the predicted limiting currents are less than the theoretical limiting currents at both low and high flow rates. At low flow rates, the bubble group is small and bubble formation is significant (see Fig. (2)). Under these conditions, the bubble formation increases the resistivity of the pore electrolyte resulting in a more ohmic control of the reaction. The bubbles accentuate the non-uniform distribution of the current and polarization. At high flow rates, both the ohmic resistance of the electrolyte and bubble formation result in a more ohmic controlled reaction and hence lower limiting current.

Figure (9) shows the effects of the flow rate on the reaction current distributions at a constant value of K = 1. The figure shows the current distributions with and without the effect of gas bubbles included in the simulation. The current distributions were determined where the cell operates at the values of the total limiting current shown in Fig. (8). In the case where the bubble formation is not included, as the flow rate decreases the reaction becomes more uniform. Note that in this case the model accounts only for the change in I_L. At low flow rate i.e., low value of I_L the reaction becomes mass transfer limited everywhere in the bed and hence the reaction is more uniform. This case, however, is similar to the case discussed in Fig. (5) at low value of I_L.

In the case where the gas formation is included in the simulation the current distributions result from the combined effects of the bubble group, Ψ and the total limiting current, I_L. In general, the reaction is more non-uniform in the case where the gas bubble is included than in the case where the gas bubble is not included. As the flow rate decreases the thickness of the bed operating at the limiting current decreases. Note that, at low flow rates, the predicted reaction thickness operating at the limiting current is overestimated in the case where the gas bubble formation is not included. At high flow rates, however, the current distributions are almost the same in both cases pointing to the low degree of bubble formation. Neglecting the effects of gas bubbles for low values of flow rates would produce erroneous results.

It is obvious that the bubble formation affects both the values of the total limiting current (see also Fig. (8)) and the current profiles within the bed. Under these conditions, one might operate the cell at relatively high flow rates to minimize the deleterious effects of the gas bubbles and also to increase the limiting currents of the electrode. However, there is a practical limit for increasing the flow rate since the limiting current is not linearly dependent on the flow rate. At high flow rates, the conversion efficiency per pass is small and recycling of the electrolyte becomes necessary to achieve high efficiency of the process.

Conclusions

A mathematical model to simulate the gas evolution reaction at flow-through porous electrodes is introduced. The model accounts for the mass transfer resistances and gas bubble formation as well as for the kinetics and ohmic resistance. The gas bubbles accentuate the non-uniform distribution of the reaction by increasing the effective resistance of the electrolyte. Mass-transfer resistance further limits the operation of the cell since a non-uniform potential can lead to mass-transfer limited current locally within the pores. Therefore, the predicted limiting current values are lower than the theoretical limiting current of the electrode. The gas bubble formation has great influence on both the values of the limiting current and on the current distributions. It is recommended to operate the cell at relatively high flow rates to decrease the effects of the gas bubbles and increase the limiting current. Using a multiple-pass process is essential to obtain

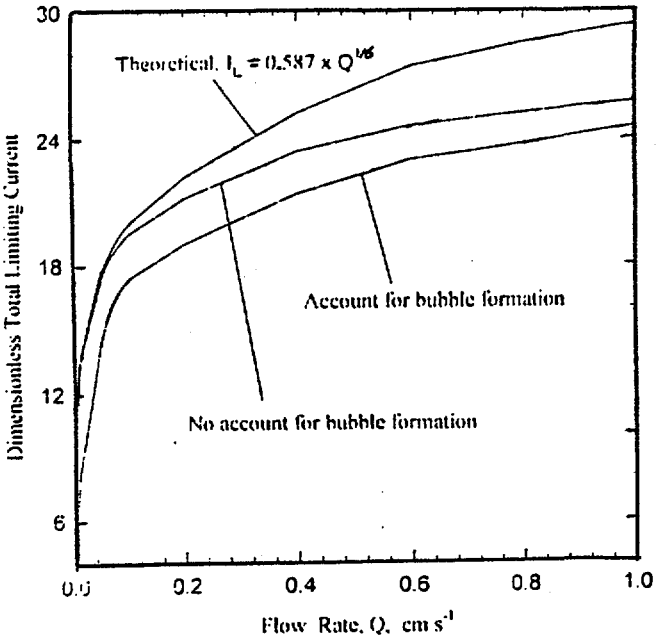

Fig. (8) Total limiting current as a function of the flow rate. K = 1; $I_o = 0.02$ A cm^{-2}.

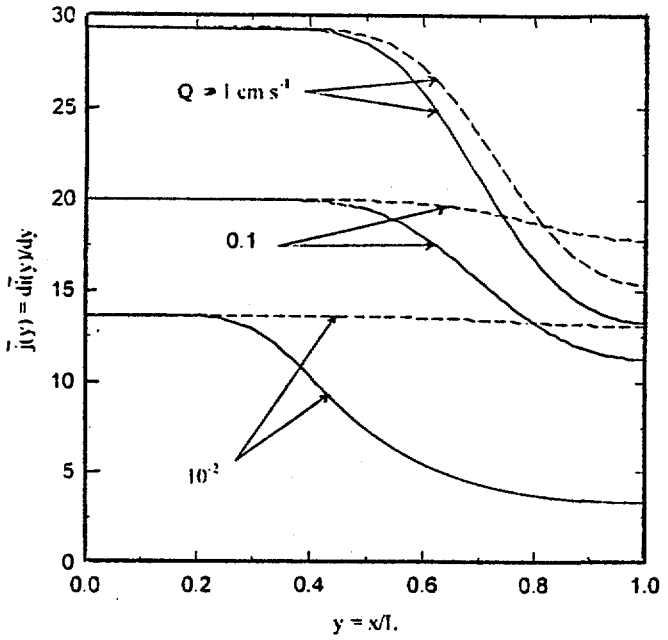

Fig. (9) Effect of the bubble formation on the reaction current distribution. The dashed lines show the cases where the bubble effects are not included and the solid lines where the bubble effects are included.
K = 1; $I_o = 0.02$ A cm^{-2}.

complete conversion.

References

1. John Dukovic and C. W. Tobias, *J. Electrochem. Soc.*, **134,** 331 (1987).
2. G. Pillay and Chao-Peng Chen, *ibid,* **143**, 3410 (1996).
3. H. Vogt in *" Comprehensive Treatise of Electrochemistry "*, Vol. **6**, (edited by J. O'M. Bockris, B.E. Conway E. Yeager and R. E. White), Plenum Press, New York (1983).
4. L. J. Janssen and G. J. Visser, *J. Appl. Electrochem.*, **21,** 753 (1991).
5. P. J. Sides in *"Modern Aspects of Electrochemistry"*, No. 18, (edited by R. E. White, J. O'M. Bockris and B. E. Conway), Plenum, New York (1983).
6. G. Kreysa and M. Kuhn, *J. Appl. Electrochem.*, **15,** 517 (1985).
7. D. H. Coleman, D. T. Hobbs and R. E. White, *J. Electrochem.. Soc.*, **142** (1995) 1152.
8. R. deLevie, in *" Advances in Electrochemistry and Electrochemical Engineering "*, Vol. **6,** (edited by P. Delahy) Wiley, New York (1967).
9. J. Newman and W. Tiedman, *" Advances in Electrochemistry and Electrochemical Engineering "*, Vol. **11,** p. 352 (edited by H. Gerischer and C. W. Tobias) Wiley, New York (1978).
10. R. E. Sioda and K. B. Keating *" Electroanalytical Chemistry "*, Vol. **12**, (edited by A. J. Bard) Dekker, New York (1982).
11. F. Goodridge and A. R.Wright in *"Comprehensive Treatise of Electrochemistry"* Vol. **6,** Electrochemical Processing, Chap. **6,** p. 293 (edited by J. O'M. Bockris, B.E. Conway E. Yeager and R. E. White), Plenum Press, New York (1984).
12. C. Oloman, *J. Electrochem. Soc.*, **126,** 1885 (1979).
13. C. L. K. Tennakoon, R. C.Bhardwaj and J.O'M. Bockris, *J. Appl. Electrochem.*, **26**, 18 (1996).
14. M. Warshy and L.O. Wright , *J. Electrochem. Soc.*, **124,** 173 (1977).
15. K. Kinoshita and S.C. Leach, *ibid.*, **129,** 1993 (1982).
16. C. Ponce De Leon and D. Pletcher, *Electrochimica Acta,* **41**, 533 (1996).
17. J. N. Bennion and J. Newman, *J. Appl. Electrochem.*, **2,** 113 (1972).
18. J. Van Zee and J. Newman *J. Electrochem. Soc.*, **124,** 706 (1977).
19. J. Wang and H. D. Dewald, *ibid.*, **130,** 130 (1983).
20. A. T. Kuhn, *J. Appl. Electrochem.*, **4,** 69 (1974).
21. Y. Oren and A. Soffer, *Electrochim. Acta,* **28,** 1649 (1983).
22. J. M. Bisang, *J. Appl. Electrochem.*, **26,** 135 (1996).
23. D. T. Chin and B. Eckert , *Plat. Surf. Finish.*, **10,** 38 (1976).
24. B. G. Ateya and B. El- Anadouli , *J. Electrochem. Soc.*, **138,** 1331 (1991).
25. B. El-Anadouli and B. G. Ateya, *J. Appl. Electrochem.*, **22,** 277 (1992).
26. M. M. Saleh, J. W. Weidner and B. G. Ateya, *J. Electrochem. Soc.*, 142 (1995) 4113.
27. P. De Vidts and R. E. White, *ibid,* **144,** 1343 (1997).
28. J. A. Trainham and J. Newman, *ibid,* **124,** 1528 (1977).
29. B. G. Ateya and L. Austin, *ibid.*, **124**, 1540 (1977).
30. B. G. Ateya, *J. Electroanal. Chem.*, 75, **183** (1977).
31. L. E. Cussler *"Diffusion and Mass Transfer"*, p. 230, Cambridge University Press (1984).
32. N. Wakao and S. Kaguei *"Heat and Mass Transfer in Packed bed"*, p. 145, Gordon and Breach Science Publishers, New York (1982).
33. C. Tobias and R. E. Meredith, in *" Advances in Electrochemistry and Electrochemical*

Engineering ", Vol. 2, (edited by H. Gerischer and C. W. Tobias), John Wiley & Sons, New York (1962).
34. J. Newman in "*Electrochemical Systems* ", p. 552, App. C, 2nd Edition, Prentice-Hall, Englwood Cliffs, New Jersey (1991).